

On the flow structure of an inclined jet in crossflow at low velocity ratios



C. Dai, L. Jia¹, J. Zhang, Z. Shu, J. Mi*

State Key Laboratory for Turbulence and Complex Systems, College of Engineering, Peking University, Beijing 100871, China

ARTICLE INFO

Article history:

Received 3 May 2015

Revised 1 December 2015

Accepted 2 December 2015

Available online 29 December 2015

Keywords:

Flow structure

Inclined jet

Low velocity ratio

Coherent structure

ABSTRACT

This study investigates the influence of different low velocity ratios on the flow structures of an inclined jet in crossflow (JICF). Experiments are conducted in a closed-loop water tunnel with a jet issuing from a round nozzle inclined at 35° with the streamwise direction of the crossflow. The flow structures are visualized using Laser Induced Fluorescence (LIF) and measured by Particle Image Velocimetry (PIV). Four velocity ratios of $VR = 0.5, 1.0, 1.5,$ and 2.0 are considered with the density ratio $\rho_j/\rho_\infty = 1$ and the Reynolds number $Re = 1712$ (based on the jet diameter and cross-flow velocity). Under the same conditions, Large-Eddy Simulations (LES) are operated for $VR = 0.5$ and 2.0 , focusing on the three-dimensional dynamics of the JICF. Predictions by LES are found to agree well with the measurements.

The qualitative and quantitative analyses suggest that the flow patterns and their unsteady behavior change with the velocity ratios considerably. When $VR = 0.5$, it is mainly hairpin vortices behaving like the classic counter-rotating vortex pair (CRVP) that dominate the JICF. As the velocity ratio increases, the classic JICF topology recovers and the ubiquitous CRVP becomes the characteristic feature of the JICF and persists far downstream for $VR = 2.0$. The LES results reveal that the coherent structures generated in the nozzle tube are initiated by the separation zone at the jet inlet sharp edge and play an important role in the formation of the hairpin vortices and the CRVP.

© 2015 Elsevier Inc. All rights reserved.

1. Introduction

The jet in crossflow refers to a jet of fluid emanating from a nozzle and interacting with the surrounding fluid that flows across the nozzle exit. This phenomenon or the like exists extensively in nature and also in many industrial applications, such as volcanic eruptions, pollutant in plumes, dilution jets in combustors, and cooling of turbine blades (Karagozian, 2014). Consequently, the control and understanding of JICF is of great industrial interest. Besides, the interaction between the jet and the crossflow generates a highly complex three-dimensional, unsteady and nonlinear flow, making it an active subject of many experimental (Kelso et al., 1995; Cambonie and Aider, 2014), theoretical (Mcguirk and Rodi, 1978; Needham et al., 1988) and numerical studies (Le et al., 2011; Coletti et al., 2013) in fluid mechanics over the past few decades (Karagozian, 2010). Detailed reviews on this subject may refer to Margason (1993) and Mahesh (2013).

Previously, most studies have been conducted on a jet initially at a right angle to crossflow. For example, Bidan and Nikitopoulos (2013) focused on the vortical structures encountered in steady and pulsed transverse jets at $0.15 \leq VR \leq 4.2$. Kelso et al. (1996) studied

the structures of normal round jets in crossflow using flow visualization techniques and flying hot wire measurements with $2.0 \leq VR \leq 6.0$. Based on the flow visualization of a round jet ejected vertically into the horizontal crossflow, Fric and Roshko (1994) documented four fundamental vortical structures involved in the JICF as shown in Fig. 1: the horseshoe vortex that forms upstream of the jet exit, the jet shear-layer formed primarily at the windward jet/crossflow interface, the counter-rotating vortex pair (CRVP) and the unsteady tornado-like wake vortices underneath the detached jet. Among them, the time-averaged defined CRVP is usually considered the most significant structure for the entrainment and mixture between the jet and crossflow.

However, the flow structures in JICF are not always those four types of vortices when the velocity ratio changes and their formation mechanisms are different as well. Mahesh (2013) concluded that the JICF structures at low velocity ratios are different from those canonically at high ones. In the low ratio regime, the interaction of the jet with the crossflow is in fact dominated by hairpin vortices. Bidan and Nikitopoulos (2013) found that, at low velocity ratios, a stable leading-edge shear-layer rollup is identified inside the jet pipe. As the velocity ratio increases, this structure becomes destabilized and forms other transverse jet vortices. Kelso et al. (1996) showed that the unsteady upright vortices in the wake may form by different mechanisms for different velocity ratios. Recently, Cambonie and Aider (2014) conducted a study that was aimed at providing a

* Corresponding author. Tel.: +861062767074; fax: +861062767074.

E-mail address: jmi@pku.edu.cn, prof.jmi@gmail.com (J. Mi).

¹ The co-first author

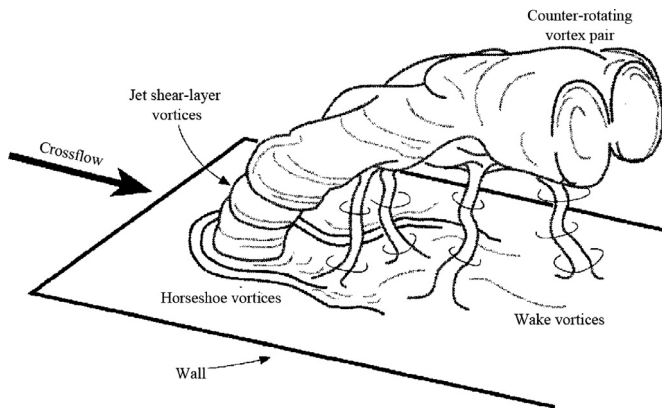


Fig. 1. Schematic illustration of vortical structures of the JICF near the jet exit (Fric and Roshko, 1994).

complete transition scenario of the JICF topology from the lowest velocity ratios to high ones ranged between 0.16 and 2.13. According to the global evolution scenario of the round JICF topology proposed, the jet is almost attached and strongly interacts with the boundary layer for $0.3 \leq VR \leq 0.6$, and it is also periodically swept by the crossflow when $VR \leq 0.3$, due to the jet momentum being not sufficiently strong to sustain a steady obstacle for the crossflow. For $VR > 1.25$, the classical JICF vortical structures sketched in Fig. 1 are recovered.

Compared to the normal JICF, the flow structures and their originations of an inclined jet into crossflow at low velocity ratios are very different. Surprisingly, the impact of low velocity ratios on the flow structures is less appreciated (Mahesh, 2013). Only a few articles have shown results on an inclined JICF for $VR \leq 2.0$, and most of them are conducted numerically. Guo et al. (2006) studied the influence of the jet inclination on the flow field. They compared a normal and a 35° stream-oriented inclined jet at low velocity ratios of 0.1–0.48 using LES. In their results, hairpin vortices are not mentioned; similar structures of recirculation, spanwise rollers at the windward jet/crossflow interface, and the counter-rotating vortex pair (CRVP) were observed for the normal and the inclined jets. At the lower velocity ratios, no horseshoe vortex was observed at the leading edge of the jet. They considered that the CRVP is originated from the shear layer of the jet/crossflow interaction and the streamwise vorticity contained in the boundary layer next to the jet exit. Tyagi and Acharya (2003) also performed an LES of a streamwise 35° round jet at low velocity ratios of 0.5 and 1, with the Reynolds number of $Re = 15,000$. Contrary to Guo et al. (2006), these investigators clearly showed the street of hairpin vortices in the wake of the jet exit and the far-field as they were convected downstream. It was concluded that the hairpin vortices were the origin of the CRVP. Recently, Fawcett et al. (2013) experimentally provided the visualization of the JICF structures and showed that the jet structure changes with the velocity ratio. The same conclusion was obtained by Sakai et al. (2014). For the CRVP origination, despite several initiation mechanisms have been proposed (Andreopoulos and Rodi, 1984; Marzouk and Ghoniem, 2007), relatively little attention has been paid to the effects of the supply plenum and nozzle flow on its development (Peterson and Plesniak, 2002; Peterson and Plesniak 2007).

In the context of the above work, the present study is designated to focus on the vortical structures associated with an inclined jet in transverse flow at low velocity ratios and relatively lower Reynolds number, by means of both experiment and numerical computation. To this end, the flow structures of several selected planes are visualized by laser induced fluorescence (LIF) and quantitatively measured by particle image velocimetry (PIV). Since the consensus that the RANS models have a poor prediction for the anisotropy JICF problem and DNS has the limitation of huge computational cost, the present modeling uses LES for the numerical work. A detailed illustration of

the flow structures for the low-velocity-ratio JICF is to be presented later for better understanding of their origination and evolution as the velocity ratio is increased, especially for the hairpin vortex and CRVP structure.

2. Apparatus and procedures

2.1. Experimental details

Experiments are performed in a closed-loop low speed water tunnel with an 6 m long test section by an $0.4 \text{ m} \times 0.4 \text{ m}$ cross-section, schematically described in Fig. 2(a). A set of five filter screens followed by a contraction with an area ratio of 2:1 is located directly upstream of the test section, removing large-scale secondary flows and providing stable inlet conditions during the experiments. The test section comprises three main parts made of acrylic: the test plate, the supply plenum and the inclined nozzle. The test plate served as boundary wall is 0.90 m (length) \times 0.36 m (width) and is installed in the mainstream zone below the air/water shear layer. The round hole is drilled streamwise-oriented 35° in a thick disk, with a diameter $D = 23 \text{ mm}$ and a length $L/D = 3.8$, classified as the low stroke ratio (Sau and Mahesh, 2008). The jet exit center is mounted $13D$ downstream of the test plate leading edge and $26D$ upstream of the trailing edge. The jet from a supply plenum ($10D$ in diameter and $6D$ in height) was fed by a secondary pump, which is monitored via a rotameter to make the velocity ratio accurate. In the supply plenum, the cells of the honeycomb are round (diameter $d = 6 \text{ mm}$) and have a length of 20 cell diameters. The coordinates X , Y and Z correspond respectively to the streamwise, spanwise and vertical directions of the flow, as shown in Fig. 2(a) (left), with the origin taken at the center of the jet exit.

The turbulence intensity of the crossflow at the test section entrance and the jet out of the honeycomb is 3% and 0.5% respectively. The main flow Reynolds number Re is 1712; where $Re \equiv U_\infty D/\nu$ with D being the jet nozzle diameter, U_∞ the bulk velocity and ν the viscosity. For different values of the velocity ratio U_j/U_∞ , the rate of the jet flow is changed by modulating the rotameter while the mainstream velocity stays constant. The working fluid is water for both the mainstream and the jet at ambient temperature, thus obtaining that the density ratio $\rho_j/\rho_\infty = 1$ and the blowing ratio $BR \equiv \rho_j U_j / \rho_\infty U_\infty = U_j/U_\infty$. As the blowing ratio scales the thermal transport capacity of the coolant, it is arguably a more important parameter than the velocity ratio which scales the turbulent production for film cooling (Coletti et al., 2013). However, we take the velocity ratio as the only variable here, since it has the same value of the blowing ratio.

Prior to the PIV measurements, LIF visualizations are conducted in both vertical and horizontal sectional planes (schematically shown in Fig. 2(b)) to obtain instantaneous tomographic images of the JICF. The jet plenum is filled with a dilute mixture of the rhodamine-6G-chloride and water. Planar sections are illuminated via a laser light sheet produced by a pulsed laser source passing through a negative-focal-length cylindrical lens. A long-focal-length cylindrical lens is used to focus the sheet, with the thickness of the light sheet being about 1 mm. The laser sheet beam is illuminated during 4 ns using a 15 mJ/pulse Nd:YAG laser, with the wavelength being 532 nm. An optical low-pass filter is used to isolate the fluorescence from the laser wavelength spectrally. The sheet is oriented to clearly view the jet trajectory and discern the vortex structures within the jet in the planes parallel and perpendicular to the plate. The fluorescence dye is supplied only into the jet flow; hence the coolant jet flow patterns are clearly recognized as the images. Fig. 2(b) shows the orthogonal planes with positions at which LIF measurements are taken. The symmetric plane (X - Z section, $Y/D = 0$) is measured to determine the trajectory of the JICF, also the windward and leeward vortical structures. For this, the laser is placed on a tripod horizontally under the water tunnel, with a mirror used to shift the light 90° . For the other planes

Download English Version:

<https://daneshyari.com/en/article/655052>

Download Persian Version:

<https://daneshyari.com/article/655052>

[Daneshyari.com](https://daneshyari.com)